15th World Congress on Computational Mechanics (WCCM-XV)
8th Asian Pacific Congress on Computational Mechanics (APCOM-VIII)
Virtual Congress: 31 July – 5 August 2022
S. Koshizuka (Ed.)

EXPERIMENTAL INVESTIGATION OF THE STATIC AND DYNAMIC BEHAVIORS OF 3D-PRINTED SHELL STRUCTURES

Raffaele Cucuzza[1]*, Alessandro Cardoni[1], Amedeo Manuello[1], Marco Domaneschi[1], Gian Paolo Cimellaro[1] and Giuseppe Carlo Marano[1]

[1] Department of Structural, Geotechnical and Building Engineering Politecnico di Torino, Corso Duca degli Abruzzi, 24 - 10129. Torino, Italy
*Corresponding author E-mail: raffaele.cucuzza@polito.it

Key words: Multy-body Rope Approach, Shape Optimization, Vaults, Static and dynamic analysis, Digital Image Correlation, Fuse Deposition Modeling

Abstract. *Over the last years, several optimization strategies were conducted to find the optimal shape minimazing internal stress or total weight (volume) of shell structures. In recent times, this structure typology gained a great importance among researchers and the scientific community for the renowed interest in the form-findind optimization of column-free space solution for large span roofing constructions. In the present paper, a form-finding of a shallow grid shells was introduced basing on the multy-body rope approach (MRA) for the definitions of vault shapes and different hole percentage. In order to obtain an experimental validation, a physical model was reproduced at the laboratory scale performing ad hoc measurements to compare the observed respect to the simulated behaviour. A 3D printing procedure based on the Fuse Deposition Modeling (FDM) technique in polylactide (PLA) material was used to realise form-works of the cement based blocks of the scaled prototype. Several static and dynamic load configurations are investigated, collecting into a sensitivity analysis the parameters which mainly affect the structural behaviour. To simulate earthquake ground motion an assigned frequency range as dynamic input to the structure was provided by a shaking table. Finally, some preliminary considerations of the dynamic response of the model were provided testing the robustness of the form-finding approach when horizontal load are taken into account.*

1 INTRODUCTION

In the last two decades, several authors have discovered new ways to use and integrated masonry structures in the actual architectural and engineering environment experiencing with innovative realisations and design tools (e.g. [1], [2], [3], [4], [5]). Due to the imminent environmental problem, new structural solutions which are able to comply the demand of sustainability with the structural efficiency are required. Moreover, thanks to the emergence of optimisation techniques (e.g. [6], [7], [8], [9], [10]), generative design and parametric analysis (e.g. [11], [12]), masonry structures has regained their leading role in the architectural and engineering field. Computer based design and modelling procedures have revolutionised the structural design concept generating holistic approaches for shape, material and structures (e.g. [11], [3]). In this field, new form-finding techniques based on automatic tools and digital fabrication methods played a fundamental role in the realisation of non-conventional and free form architectures. In order to provide innovative structural and architectural solution, visual representation (e.g. [1], [5]) and real-time reaction (e.g. [1], [13]) of buildings information have assumed a crucial role. Therefore the increasing interest to study ancient masonry vaults, erected all over the world, is due to the

stability condition of this specified structural topology and for their chip extraction operation cost of raw material.
In the last decades, the problem of doubly-curved shells (e.g. [13]) and either curved surface design, taking into account the fixed framework of funicular or compression-only vault design, are widely covered by most authors (e.g. [1], [14], [15], [16]). Moreover, first works in this field have been based on hanging models and graphic statics for investigating domed structures.
At the beginning of the 20th century, the first to deal hanging scaled reproductions in the design process of the Crypt of Colònia Güell was Antoni Gaudí as widely discussed in [1] and [13]. Then, Frei Otto approached hanged models to detect the form for the lattice shell in Mannheim [15] or Swiss engineer Heinz Isler who faced for the first time a compression-only concrete shell realised using hanged cloth mockups (e.g. [1], [17]).
Recently, new developed optimisation techniques applied on grid shells has been carried out with the aim to find the optimal configuration in terms of topology, shape and size of the members composing it (e.g. [18], [19]). Optimisation is the procedure of finding the minimum or maximum value of a function by choosing a number of variables subject to a number of constraints.
The optimising procedures mentioned above has been applied in several fields as tension and compression-only trusses [20], high-rise buildings [21] or highway and railway trussed bridge [22] and using different problem formulations and optimisation statements like truss topology method [23], graph based design [24], simulated annealing [25] and cut-and-branch methods [26].
One of the most recent techniques that has found wide use in the recent literature is the genetic algorithm belonged to the macro-field of the Evolutionary algorithm. In this approach the principle of natural selection to evolve a set of solutions towards an optimum solution is used (e.g. [27]). Several investigation using this efficient population-based algorithm have been provided with the aim to find the optimal shape configuration of three-dimensional discrete system, such as spatial structures, planar structures and geodetic domes [28].
Other popular approach for multi-objective optimisation is proposed by Pareto [29]. A solution is Pareto optimal or non-dominated when no other feasible solution that improves one objective without deteriorating at least another one occurs. A popular method based on detecting the best shape and topology configuration is the Form-finding approach in which force density method [26] and the dynamic relaxation (DR) [28] are employed.
Among the last kinds of system mentioned above, Kilian and Ochsendorf [30] developed a shape-finding tool for statically determined systems based on particle-spring model. Following this new shape-finding trend, Block and Ochsendorf proposed the thrust network analysis in order to detect the optimal shape which guaranteed pure compression action on each truss, especially for masonry structures [31]. Each approach or algorithm proposed above have both advantages and disadvanteges. To overcame the limits of these models, hybrid approach have been proposed coupling form-finding and grid optimisation as widely discussed by Richardson et al. in [32].

In the present paper, the shape of the vault model is principally obtained by a form-finding method fine-tuned by one of the authors [14][7]. The peculiarity of this method lies in the adaptability regards cases of free shapes with standardised constituting elements. One of the purposes of this work, in fact, is to propose an evaluation not only on the goodness of the form finding method adopted but also considering the best solution among the different pattern of the pierced configurations (disposition of the holes). Different funicular structures have been analysed in order to recognise the best shape together with the most efficient hole pattern configuration.

The final geometric configuration of the vault is obtained by analysing the effect of some chosen parameters such as the lowering degree (defined as the ratio between the maximum span D and h, defined as the height of the vault), the slack coefficient of the original hanging net and the hole percentage (HP) of the covering surface. The final shape and the pierced pattern were analysed by the MidasGen©software under static and seismic load pattern configuration once constraint conditions were fixed.
Manufacturing process, [33], was adopted with the aim to achieving a scaled prototype of the selected vault typology. Moreover, a geometric survey was necessary to obtain, with a certain level of confidence, the input geometric data for numerical analysis as *Mechanical Autocad*©3d Model of the scaled-prototype.
Incremental static and linear dynamic analysis with direct integration of the equations of motion are performed in order to evaluate, given a starting configuration, the gap between the expected structural response and the observed one into the laboratory in terms of stress, deflections and natural frequency. To do that, once the results are obtained by numerical analysis, a target point was selected for either static and dynamic configuration in order to prepare final comparisons. The same target point will be investigated in the scaled-prototype vault adopting 3D Digital Image Correlation (DIC) technique under loading in order to recognize the pattern deformation. DIC technique, in particular, is almost largely used by researchers and engineers to evaluate the stability and the collapse condition of these kinds of structures using full-field quantitative measurement of motions and deformations. This measures are based on a mapping process of the investigated area by image registration and tracking methods for accurate 2D measurements of changes in images. Algorithms working on mutual correlation between different pictures, it is able to detect dissimilarities before and after deformation and, adopting refined statistical functions, typical deformation of the vault corresponding to different level of damage or loading condition are recognized.
Finally, some preliminary results obtained by static and dynamic analysis are discussed.

2 SHAPE OPTIMIZATION USING FORM-FINDING TECNIQUES

At first, numerical analysis were performed with the aim to adopt form finding procedures for each investigated shape configuration. For a free form compressed vault, a squared geometry (16×16 m^2) is selected with varying suitable parameters:the lowering degree (D/h) and the hole percentage (HP). The form-finding approach adopted in the paper was originally presented by one of the authors in 2004 [34] and was successively revised and expanded concerning to the original idea [14].
Adopting the MRA approach, several disparate forms of a hanging lattice constituted by spherical masses joined by flexible ropes were found when dynamic simulation in the time domain are performed [34]. Hence a step-by-step procedure can be performed considering either different load cases and both 2D and 3D systems.
The such named multi-bodies rope approach (MRA) mentioned above is capable of making the hanged mesh, for a precise group of masses, in order to create the final 3D funicular state [14]. The investigated suspended net with standard MRA is composed by nodes and ropes and in particular a generic node "i" of the grid with quadrilateral mesh is examined. At this node a number j of ropes (such as 4: a, b, c, d) are converging. At the same time, s_j represents the forces inside them. The node "i" is identified by the coordinates u_i, v_i, n_i. The investigated load pattern adopted by performing analysis very often coincident with the self-weight simulated by the mass at each sphere. The equilibrium at each node of the suspended net is ensured by the following equation [34] in which velocity and the acceleration are in

proportional ratio:

$$R_i = \sum_{k=1}^{N} s_j + \sum_{k=1}^{N} 2p_m + f^I + f^{II} = 0 \tag{1}$$

where, as

- R_i was the resultant in the node i at each step;
- f^I was the inertial force with a module equal to the product between the mass of the node and the amplitude of the acceleration vector with a verse equal to the opposite verse of the acceleration itself;
- f^{II} was the dissipative force assumed equal to the product of a constant times the velocity vector with a direction equal to the opposite of the velocity itself;
- s_j represented the forces in the ropes converging in the node i;
- The indexes n and n2 are, respectively, the number of the ropes converging in the node and the external loads applied on the same node.

The convergence of the system was guaranteed thanks to the physical process of the three-dimensional suspended grid. In this case, a non-linear system of equations depending by local coordinates u, v and n can be provided and the final solution can be achieved by numerical methods (see [34] and [35]).
Adopting this frame, the solutions are found managing dynamic balance equation which have been solved trough step-by step analysis [14]. Hence, velocity and acceleration have been expressed in explicit form as evidenced in [14] and [35]):

$$u'(x) = \frac{\partial u}{\partial t}; \qquad v'(x) = \frac{\partial v}{\partial t}; \qquad n'(x) = \frac{\partial n}{\partial t} \tag{2}$$

$$u''(x) = \frac{\partial u'}{\partial t}; \qquad v''(x) = \frac{\partial v'}{\partial t}; \qquad n''(x) = \frac{\partial n'}{\partial t} \tag{3}$$

The equations are written depending by u, v and n respectively along x, y and z directions. Due to the large number of variables of the model, the author adopted a numerical approach to solve the system by a multi-bodies numerical inspired by Runge-Kutta's solution method.
To overcome the increase due to the large-size research domain, a preliminary design of the grid has been detected using NURBS (Non Uniform Rational Basis-Splines) surfaces working within the MRA approaches. At the final stage, the reversed model corresponding to the final step (equilibrium step) of the hanging net is obtained.
Substantially, the main peculiarity of the method herein adopted (MRA) lies on the inextensibility property of the rope elements composing the suspended model. Due to this fact, only tension stress are supported by the elements thought very complex loading (vertical and horizontal concentrated or distributed pattern) configuration are acting on the reversed grid. In the overturned configuration, in fact, compressed-only elements are detected and well-defined length for each beams composing the grid is defined.
In the present paper, taking into account that the form-finding was used to define compression-only vault optimal shapes, the geometries obtained by the MRA were also validated by the MidasGen©software in order to obtain a validation of the funicular shapes. The model used for the numerical simulation in MidasGen©will be widely discuss in the next section dedicated to the scaled-prototype realization of the vault 3. The entire model results full-constrained at the four corner points as fixed joints on the ground supporting the vault. A FEM parametric analysis is conducted with the aim to define the parameters that

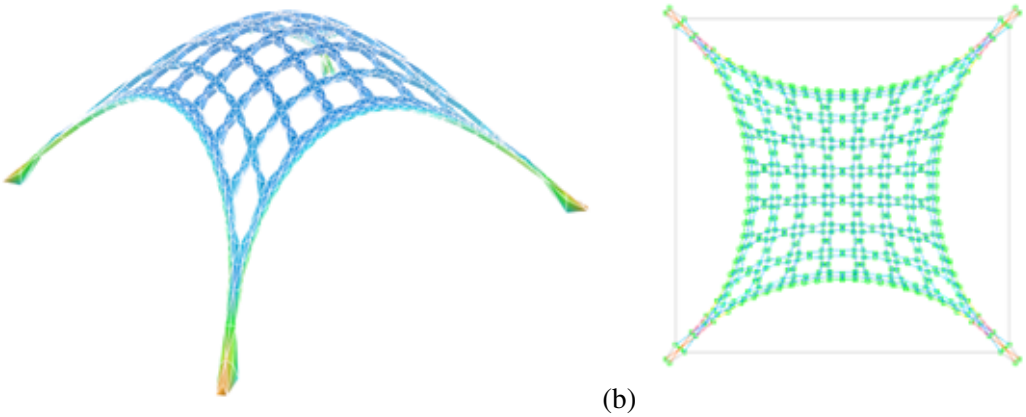

(a) (b)

Figure 1: Final configuration obtained by form-finding technique when maximum pierced area percentage of 45.46% is achieved. (a): Axonometric view. (b): top view

most affected the form-finding procedure.
With the aim to fulfill the refurbishment criteria of existing masonry vaults in which the enlarged necessity to increase openings for natural light occurs, amount of the holes (hole percentage: HP) and the positions of these openings (pattern) are chosen as main and crucial parameters for subsequent analysis. Moreover, material saving approach is almost widely adopted in the practice design for several kind of structures. Specifically, topology optimization, in fact, is increasingly used for pierced vault topology to minimize the structure's total self-weight by varying the most relevant parameters selected by a preliminary sensitivity analysis (see Figure 1).

3 SCALED-PROTOTYPE REALIZATION OF THE VAULT AND GEOMETRIC SURVEY

In order to validate the form-finding procedure using MRA approach a scaled-prototype of the reverse suspended net was realized.
The total height is equal to 30 cm. The measures previously mentioned have been subjected to a scaling procedure with a scaling factor equal to 0.0625 (1/16) in order to have the side equal to 1 m. Following this procedure, the scaled-prototype vault was 469 mm tall with a transverse section of 18.75 mm and slenderness equal to 80.
The entire vault was divided in suitable bricks composing the rods of the grid structure. As depicted in 2, each form-work corresponds to a specific brick and a sequential numbering of the bricks was adopted for the final assembling phase. This phase is of crucial importance for success by analizing the global behaviour of the structure under well-defined load pattern.
Using rapid prototyping tool-kits, the shape of the vault was separated in several dowels. The bricks have to be realized in mortar cement so a mould system has to be designed. Due to the small scale of the model, it is very important to ensure the accuracy of the formwork geometry. To achieve this purpose, the geometry of each formwork was designed into Rhinoceros using the parametric computer aided-design software Grasshopper. Hence, once the geometric features of the moulds was obtained, they have been transferred as input data to a 3D Bio-printer with a Fuse Deposition Modeling (FDM) technique in PLA material (completely eco-friendly). The most relevant parameters set up for the 3D printing process are:

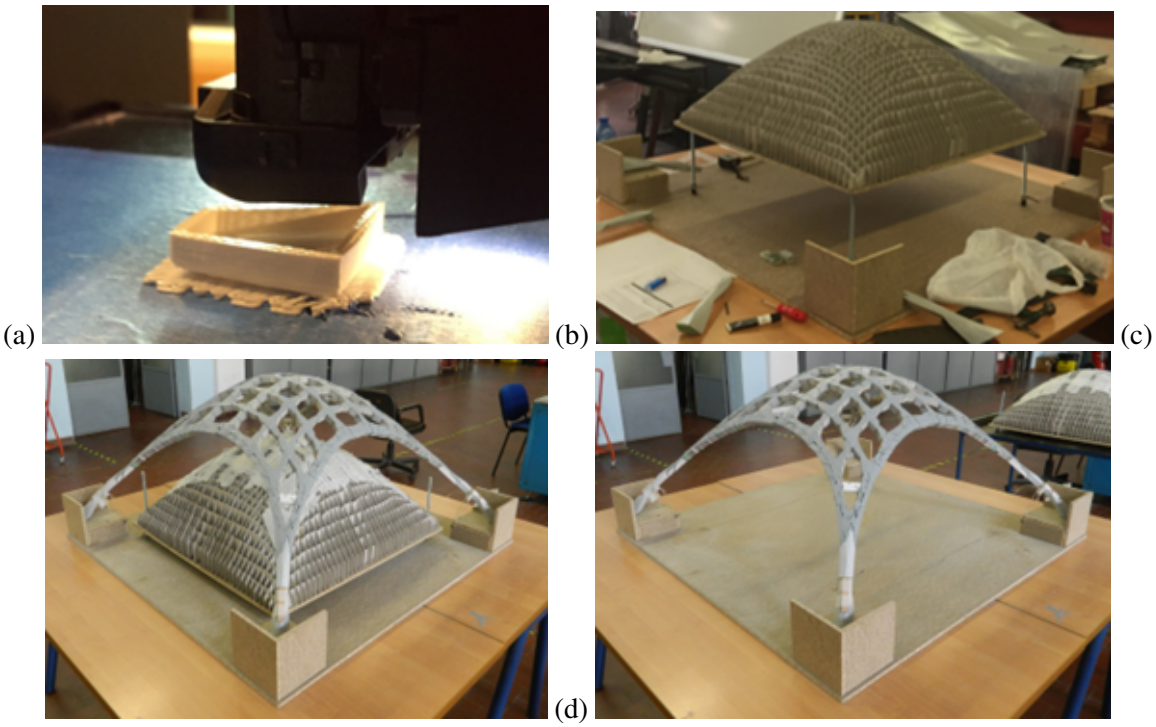

Figure 2: the step-by-step 3D printing procedure: (a) Formwork printing with FDM. (b) Cardboard spar was realized as supporting the prototype during the assembling phase of the vault. (c) Removing phase of the temporary supports. (d) prospective view of the self-supporting structure

a filament diameter of 1.75 mm a layer height: 0.2 mm, a fill density of 30% (see 2). At the same time the print speed was between 80–150 mm/s with a printing temperature of 215 C°. It is remarked that for the sake of simplicity the four base elements have been fabricated with the FDM technique. All bricks were cast into the shuttering and made by cement mortar with a 0.4 water to cement ratio. In Figure 2 all the construction stages are reported with a explaining caption for each one. In order to perform a FEM analysis for detecting in accuracy way the static and seismic global behavior of the real structure a geometric survey of the scaled prototype was made. All the measures concerning the point of the grid was associated to x and y coordinates in the plane and z for the height in the vertical plane. All these geometric and sectional information of each member of the vault was measured using a Leica LASER DISTO D2 (complying with Standard ISO 16331-1.). An axonometric view of the vault obtained by geometric survey is reported reported in Figure 3.

4 STATIC AND DYNAMIC ANALYSIS USING MIDASGEN ©

In this section, the numerical analysis under static and dynamic loads of the selected vault for the experimental validation is reported. The accuracy of the adopted modelling strategy will be crucial for comparison purposes between the numerical model and the experimental one. The entire vault was modelled adopting 125 beam elements to simulate the structural compression-only membrane state of the structure. The external boundary constraints are modelled as spherical hinges (see Figure 4). To perform static analysis, six sequential loading steps were considered and the total load, for each step, is

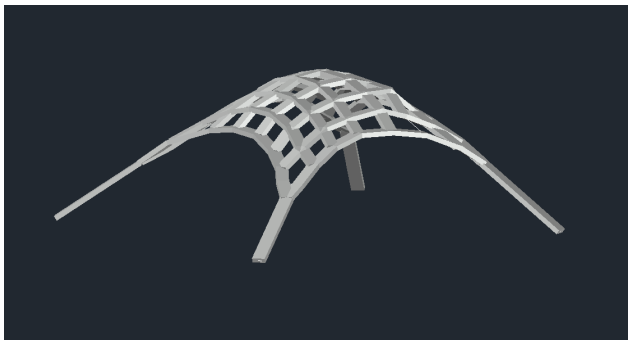

Figure 3: Axonometric view of the 3D Geometrical Model obtained by geometrical survey

(a) 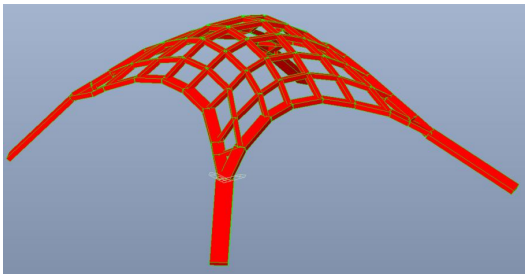 (b) 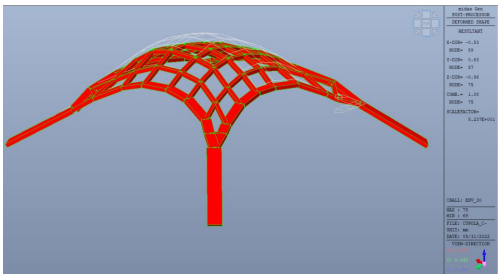

Figure 4: (a) 3D solid model of the vault obtained by MidasGen©. (b) Displacement plot concerning the critical load configuration corresponding with the last loading step (Total external load equal to 24 kg)

Table 1: Set-up and results of the numerical analysis

Loading step	ext. load $[kg]$	ext. load/Tot. weight $[\%]$	Displacement by numeric analysis $[mm]$	Tot. weight $[kg]$
1	16	211	0.51	7.59
2	32	422	1.02	
3	48	633	1.53	
4	64	844	2.04	
5	80	1054	2.55	
6	96	1265	3.1	

expressed as percentage of the total weight of the structure as reported in Table 1. The loading procedure is obtained applying concentrated nodal loads which will be implemented in the experimental model through water reservoirs. The mechanical properties of the vault and the load patterns (reference to the Figure 13 in [14] for the application point of loads) are those already described in a previous work of one of the authors ([36]). Table 1 reports the displacement field for each loading step.

In this phase, a Linear Dynamic Analysis with direct integration of the equations of motion has been

Table 2: Results of the eigenvalue analysis and modal partecipation masses printout

Mode	Frequency $[Hz]$	Transl. - X $[\%]$	Sum - X $[\%]$	Transl. - Y $[\%]$	Sum - Y $[\%]$	Transl. - Z $[\%]$	Sum - Z $[\%]$
1	22.15	34.25	34.25	5.04	5.04	7.08	7.08
2	23.05	10.69	44.94	30.19	35.23	2.56	9.64
3	26.13	1.85	46.78	12.56	47.79	2.87	12.50
4	41.17	7.36	54.14	0.01	47.80	4.34	16.84
5	52.91	0.03	54.17	6.00	53.80	2.08	18.93
6	56.60	0.23	54.40	0.02	53.81	0.96	19.89
7	60.75	1.99	56.39	0.04	53.86	0.79	20.68
8	62.47	1.98	58.37	0.53	54.38	0.03	20.70
9	104.75	0.27	58.64	0.07	54.46	9.22	29.92
10	116.92	2.89	61.53	0.95	55.41	5.51	35.43
11	136.80	2.03	63.56	1.70	57.11	1.23	36.66
12	146.99	2.99	66.55	1.65	58.76	3.88	40.54
13	210.71	0.07	66.62	3.36	62.12	53.16	93.70
14	262.57	0.08	66.70	29.06	95.18	0.04	93.74
15	280.50	28.41	95.11	0.00	95.18	0.62	94.36

performed. Preliminarily, the natural vibration modes of the structure have been computed and the first 15 vibration modes are considered as the more significant. This type analysis is preferred to assess the seismic effect on a structure when the seismic response of the structure is significantly affected by superior vibration modes. Moreover, according to the European Standard Regulation, the sum of the percentage participation mass of the 15 vibration modes, adopted for the analysis, must be higher then 85%. In order to check if the previous requirement is fulfilled by the structure, a Ritz-vector modal analysis was performed and the first 15 vibration modes are reported in Table 2 for only X, Y and Z translation vibration mode of the structure. As shown in table 2, the higher modal participation masses in percentage are reported by mode 1 and 2 for the translation mode along X, Y direction with the exception of the translation mode along Z in which the higher value is recognized for mode 13. For each translation and rotation modes the total mass participation obtained as a sum of the participation mass for each vibration mode is largely higher than 85%.

The seismic input adopted for the numerical analysis is El Centro record (North–south component of horizontal ground acceleration recorded at the Imperial Valley Irrigation District substation, El Centro, California, during the Imperial Valley earthquake of May 18, 1940). With the aim to simulate the effect of the seismic action acting on the scaled-model vault, a scale factor equal to $\sqrt{L_s/L_m} = 4$ (see e.g. [37]) was applied to the unit (Figure 5), where

- L_s is the length in the real structure;
- L_m is the length of the model .

The shaking table that will be used for laboratory experiments is uniaxial and uses two actuators placed in parallel of electro-mechanical type. Each is capable of developing a peak force of 22 kN. The vibrating plate is currently under development for the control part, while the mechanical frame is composed of reinforced steel profiles on which the actuators are installed. Figure 6 shows the 3D model of the vibrating table design and the frame installed in the laboratory at DISEG of the Politecnico di

(a) 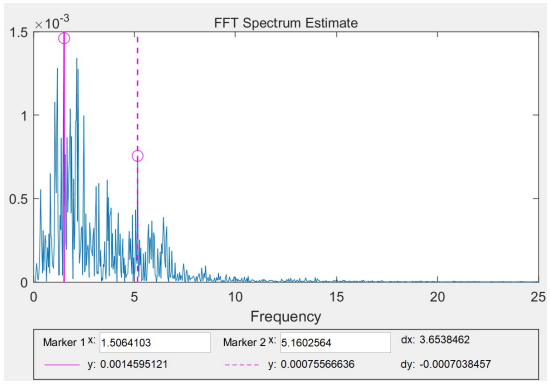

(b) 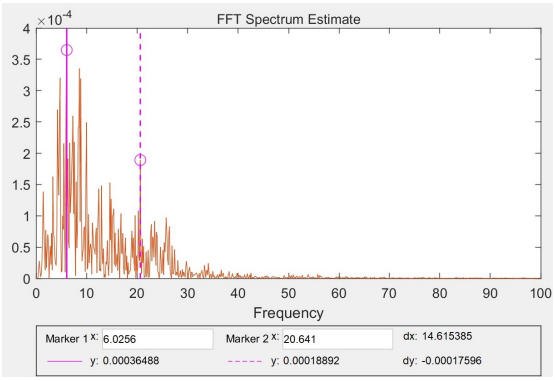

Figure 5: (a) Spectrum Estimate of El Centro record and (b) of the shaking table scale record.

(a) 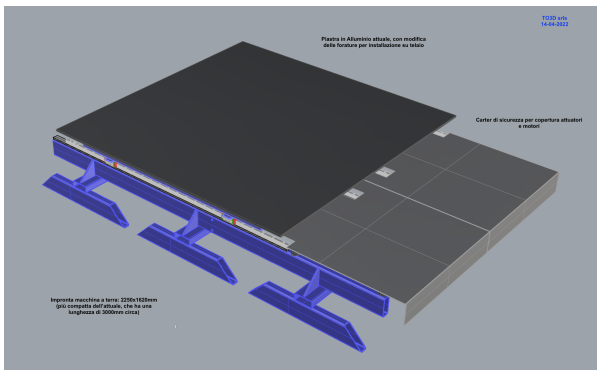

(b) 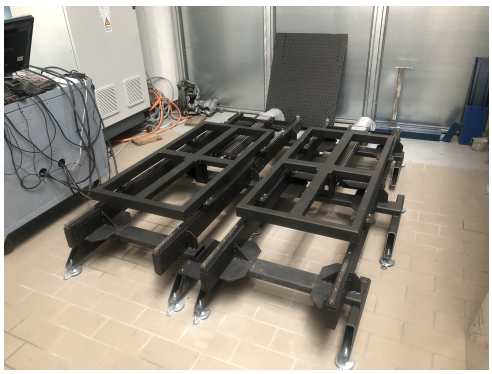

Figure 6: (a) 3D solid model of the uniaxial shaking table. (b) Shaking table frame in laboratory.

(a) 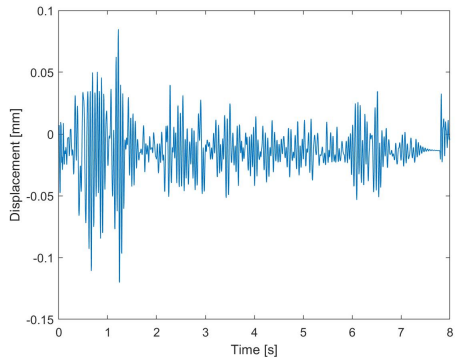

(b) 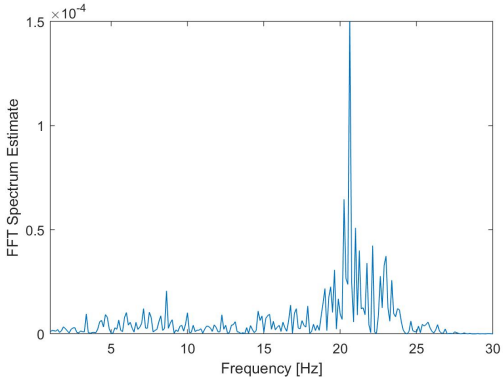

Figure 7: (a) Displacement Time-History plot of the vault top-target node. (b) Plot of the FFT Spectrum estimation. It can be observed that the pick value is found in correspondence to the first natural frequency of the vault calculated by eigenvalue analysis

Torino (Disaster Resilience Simulation Laboratory - DRSIL).

5 CONCLUSIONS

In this work, the MRA form-finding approach is adopted and the optimal shape of an only-compression vault is investigated. Static analysis with successive loading steps and Linear Dynamic Analysis with direct integration of the equations of motion was performed. Linear static analysis are performed for different loading levels with the aim to provide a validated FEM model useful for future comparisons with laboratory results. Subsequently, the dynamic response of the top of the vault in the direction parallel to the applied ground motion Earthquake component is plotted in either time and frequency domains (see Figure 7).The frequency domain outcome highlights the first natural vibration frequencies in the range 20-24 Hz accordingly with the results obtained by eigenvalue analysis. The well-know ground motion adopted for the numerical analysis is El Centro and a scale-factor is applied following the Froude theory. In future developments, the authors are going to complete the static and dynamic laboratory tests in order to assess if the form-finding procedure and the modelling strategies adopted are suitable to predict the seismic response of the scaled-prototype vault.

REFERENCES

[1] Rippmann, M., Lachauer, L., & Block, P. (2012). Interactive vault design [cited By 80]. *International Journal of Space Structures*, *27*(4), 219–230. https://doi.org/10.1260/0266-3511.27.4.219

[2] Oxman, R., & Oxman, R. (2010). The new structuralism [cited By 22]. *The New Structuralism: Design, Engineering and Architectural Technologies*.

[3] Tessmann, O. (2008). *Collaborative Design Procedures for Architects and Engineers*.

[4] Ferguson, E. (1977). The mind's eye: Nonverbal thought in technology [cited By 218]. *Science*, *197*(4306), 827–836. https://doi.org/10.1126/science.197.4306.827

[5] Kilian, A. (2006). Design exploration through bidirectional modeling of constraints [cited By 63]. *Design Exploration Through Bidirectional Modeling of Constraints*.

[6] Marano, G. C., Trentadue, F., & Greco, R. (2006). Optimum design criteria for elastic structures subject to random dynamic loads. *Engineering Optimization*, *38*(7), 853–871.

[7] Marano, G. C., Trentadue, F., & Petrone, F. (2014). Optimal arch shape solution under static vertical loads. *Acta Mechanica*, *225*(3), 679–686.

[8] Rosso, M. M., Cucuzza, R., Aloisio, A., & Marano, G. C. (2022). Enhanced multi-strategy particle swarm optimization for constrained problems with an evolutionary-strategies-based unfeasible local search operator. *Applied Sciences*, *12*(5). https://doi.org/10.3390/app12052285

[9] Cucuzza, R., Rosso, M. M., & Marano, G. (2021). Optimal preliminary design of variable section beams criterion. *SN Applied Sciences*, *3*. https://doi.org/10.1007/s42452-021-04702-5

[10] Cucuzza, R., Costi, C., Rosso, M. M., Domaneschi, M., Marano, G. C., & Masera, D. (0). Optimal strengthening by steel truss arches in prestressed girder bridges. *Proceedings of the Institution of Civil Engineers - Bridge Engineering*, *0*(0), 1–21. https://doi.org/10.1680/jbren.21.00056

[11] Cucuzza, R., Rosso, M. M., Aloisio, A., Melchiorre, J., Giudice, M. L., & Marano, G. C. (2022). Size and shape optimization of a guyed mast structure under wind, ice and seismic loading. *Applied Sciences*, *12*(10). https://doi.org/10.3390/app12104875

[12] Melchiorre, J., Bertetto, A. M., & Marano, G. C. (2021). Application of a machine learning algorithm for the structural optimization of circular arches with different cross-sections. *Journal of Applied Mathematics and Physics*, *9*(5), 1159–1170.

[13] Tornabene, F., & Viola, E. (2013). Static analysis of functionally graded doubly-curved shells and panels of revolution [cited By 154]. *Meccanica*, *48*(4), 901–930. https://doi.org/10.1007/s11012-012-9643-1

[14] Manuello, A. (2020). Multi-body rope approach for grid shells: Form-finding and imperfection sensitivity [cited By 8]. *Engineering Structures*, *221*. https://doi.org/10.1016/j.engstruct.2020.111029

[15] Burkhardt, B., & Bächer, M. (1978). *Multihalle Mannheim, Institute for Lightweight Structures (IL)*, *13*.

[16] Regalo, M., Gabriele, S., Salerno, G., & Varano, V. (2020). Numerical methods for post-formed timber gridshells: Simulation of the forming process and assessment of r-funicularity [cited By 4]. *Engineering Structures*, *206*. https://doi.org/10.1016/j.engstruct.2019.110119

[17] Chilton, J. (2000). The engineer's contribution to contemporary architecture: Heinz isler [cited By 93]. *The Engineer's Contribution to Contemporary Architecture: Heinz Isler*.

[18] Pedersen, P. (1973). Optimal joint positions for space trusses. [cited By 56]. *ASCE J Struct Div*, *99*(St12), 2459–2476.

[19] Gil, L., & Andreu, A. (2001). Shape and cross-section optimization of a truss structure [cited By 89]. *Computers and Structures*, *79*(7), 681–689. https://doi.org/10.1016/S0045-7949(00)00182-6

[20] Roy, S., & Kundu, C. (2020). State-of-the-art review on the use of optimization algorithms in steel truss. *International Journal of Scientific and Technology Research*, *9*(3), 160–165.

[21] Azad, S. K., & Aminbakhsh, S. (2021). High-dimensional optimization of large-scale steel truss structures using guided stochastic search. *Structures*, *33*, 1439–1456.

[22] Li, H., Liu, S., Shan, Q., Zhang, L., & Wu, B. (2019). Investigation and optimization of the cable force of a combined highway and railway steel truss cable-stayed bridge in completion state. *Vibroengineering Procedia*, *28*, 217–222.

[23] Beckers, M., & Fleury, C. (1997). A primal-dual approach in truss topology optimization [cited By 36]. *Computers and Structures*, *64*(1-4), 77–88. https://doi.org/10.1016/s0045-7949(96)00144-7

[24] Giger, M., & Ermanni, P. (2006). Evolutionary truss topology optimization using a graph-based parameterization concept [cited By 46]. *Structural and Multidisciplinary Optimization*, *32*(4), 313–326. https://doi.org/10.1007/s00158-006-0028-8

[25] Lamberti, L. (2008). An efficient simulated annealing algorithm for design optimization of truss structures [cited By 197]. *Computers and Structures*, *86*(19-20), 1936–1953. https://doi.org/10.1016/j.compstruc.2008.02.004

[26] Rasmussen, M., & Stolpe, M. (2008). Global optimization of discrete truss topology design problems using a parallel cut-and-branch method [cited By 55]. *Computers and Structures*, *86*(13-14), 1527–1538. https://doi.org/10.1016/j.compstruc.2007.05.019

[27] Sampson, J. R. (1976). Adaptation in natural and artificial systems (john h. holland).

[28] Toğan, V., & Daloğlu, A. (2006). Optimization of 3d trusses with adaptive approach in genetic algorithms [cited By 106]. *Engineering Structures*, *28*(7), 1019–1027. https://doi.org/10.1016/j.engstruct.2005.11.007

[29] Ngatchou, P., Zarei, A., & El-Sharkawi, A. (2005). Pareto multi objective optimization. *Proceedings of the 13th International Conference on, Intelligent Systems Application to Power Systems*, 84–91.

[30] Killian, A., & Ochsendorf, J. (2005). Particle-spring system for structural form finding [cited By 3]. *J Int Assoc Shell Spatial Struct*, *45*(147).

[31] Block, P., & Ochsendorf, J. (2007). Thrust network analysis: A new methodology for three-dimensional equilibrium [cited By 259]. *Journal of the International Association for Shell and Spatial Structures*, *48*(155), 167–173.

[32] Richardson, J., Adriaenssens, S., Filomeno Coelho, R., & Bouillard, P. (2013). Coupled form-finding and grid optimization approach for single layer grid shells [cited By 68]. *Engineering Structures*, *52*, 230–239. https://doi.org/10.1016/j.engstruct.2013.02.017

[33] Post, D. (1983). Moiré interferometry at vpi su [cited By 57]. *Experimental Mechanics*, *23*(2), 203–210. https://doi.org/10.1007/BF02320411

[34] Manuello Bertetto, A. (2004). *Lightweight Structures Resisting by Form: The Grid Shells (in Italian)*.

[35] Spagnolo, G., Paoletti, D., Ambrosini, D., & Guattari, G. (1997). Electro-optic correlation for in situ diagnostics in mural frescoes [cited By 20]. *Pure and applied optics*, *6*(5), 557–563. https://doi.org/10.1088/0963-9659/6/5/007

[36] Bertetto, A. M., & Riberi, F. (2021). Form-finding of pierced vaults and digital fabrication of scaled prototype. *Curved and Layered Structures*, *8*(1), 210–224.

[37] Bairrão, R. (2008). Shaking table testing. In O. S. Bursi & D. Wagg (Eds.), *Modern testing techniques for structural systems: Dynamics and control* (pp. 165–196). Springer Vienna. https://doi.org/10.1007/978-3-211-09445-7_4